BMC Medical Informatics and Decision Making

RESEARCH

Open Access

A novel method for assessing cycling movement status: an exploratory study integrating deep learning and signal processing technologies

Yingchun He[1,2], Yi-haw Jan[3,4], Fan Yang[1,5], Yunru Ma[1] and Chun Pei[1,5*]

Abstract

This study proposes a deep learning-based motion assessment method that integrates the pose estimation algorithm (Keypoint RCNN) with signal processing techniques, demonstrating its reliability and effectiveness. The reliability and validity of this method were also verified.Twenty college students were recruited to pedal a stationary bike. Inertial sensors and a smartphone simultaneously recorded the participants' cycling movement. Keypoint RCNN(KR) algorithm was used to acquire 2D coordinates of the participants' skeletal keypoints from the recorded movement video. Spearman's rank correlation analysis, intraclass correlation coefficient (ICC), error analysis, and *t*-test were conducted to compare the consistency of data obtained from the two movement capture systems, including the peak frequency of acceleration, transition time point between movement statuses, and the complexity index average (*CIA*) of the movement status based on multiscale entropy analysis.The KR algorithm showed excellent consistency ($ICC_{1,3}$=0.988) between the two methods when estimating the peak acceleration frequency. Both peak acceleration frequencies and *CIA* metrics estimated by the two methods displayed a strong correlation ($r > 0.70$) and good agreement ($ICC_{2,1}$>0.750). Additionally, error values were relatively low (MAE = 0.001 and 0.040, MRE = 0.00% and 7.67%). Results of *t*-tests showed significant differences ($p = 0.003$ and 0.030) for various acceleration *CIAs*, indicating our method could distinguish different movement statuses.The KR algorithm also demonstrated excellent intra-session reliability (ICC = 0.988). Acceleration frequency analysis metrics derived from the KR method can accurately identify transitions among movement statuses. Leveraging the KR algorithm and signal processing techniques, the proposed method is designed for individualized motor function evaluation in home or community-based settings.

Keywords Deep learning, Keypoint RCNN, Inertial measurement unit, Time–frequency analysis, Multiscale entropy analysis, Cycling movement

*Correspondence:
Chun Pei
rockoldies@fjmu.edu.cn
[1]Department of Rehabilitation Medicine, School of Health, Fujian Medical University, Fuzhou 350122, China
[2]Department of Rehabilitation Medicine, Heyuan People's Hospital, Heyuan 517001, China
[3]Department of Transportation Engineering, Xiamen City University, Xiamen 361008, China
[4]Digital Twin Intelligent Transportation Maintenance Engineering Research Center of Xiamen City University, Xiamen, China
[5]Rehabilitation Engineering, Fujian University Engineering Research Center, Fuzhou 350122, China

Introduction

Therapist/Physician use motor function assessment methods to determine a patient's functional abilities and develop personalized training plans. Physical function assessment and training effect evaluation approaches consist of three main categories. The first is traditional scale-based methods, which are complex in quantitative analysis and rely on clinicians' experience and knowledge [1]. The second use high-end optical motion capture equipment, such as reflective marker-based 3D motion capture systems. Nonetheless, these systems are in research laboratories, and the makers are complex to be attached to a patient's skin and restrict patients' mobility. Therefore, they are unsuitable for clinical, community, or home-based scenarios [2]. Approaches belonging to the third category utilize skeletal point tracking technology based on video analysis, such as Microsoft's Kinect [3], which is affected by environmental factors.

With the widespread use of deep learning technology, more and more research applies deep learning-based algorithms to analyze human movement characteristics with recorded human action images and videos. The deep learning-based human motion analysis algorithm has the advantages of simplicity, real-time performance, and high accuracy [4]. For example, OpenPose [5] has been applied in balance assessments, fall predictions, gait analyses, and rehabilitation training [6–9]. However, it requires tremendous calculations and exhibits limited precision when capturing dynamic motions. Keypoint RCNN (KR) is PyTorch model, adding a key point detection branch to Mask-RCNN [10] and trained. It can recognize a moving body and provide 17 skeletal key points. Compared with OpenPose, it's editable and faster. However, the reliability and validity of using the KR algorithm to analyze human movement have not been determined yet.

Key point-based movement angle features are used in signal validity testing [11, 12], but need two synced smartphones for 3D data, complicating home monitoring. Acceleration can describe the human movement status well and is easy to collect. However, previous studies have not discussed the feasibility of using the KR algorithm to assess human body movement acceleration characteristics. We converted KR's displacement data to acceleration for analysis, different from angle-based methods, to explore a new motion assessment method. Thus reducing the computation process on the movement analysis.

Kinematic data's time-frequency features can use Fourier Transform (FT) and Short-Time Fourier Transform (STFT) reflect human motion information. Nonlinear entropy like multiscale entropy (MSE) [13] measures data complexity, good at single/multiple scale changes. Within a certain range, higher entropy means more complex. MSE on surface electromyography can measure lower limb muscle fatigue [14], suggesting it can be a feasible method for extracting fatigue features.

Fatigue causes physical/mental changes and increases injury risk in rehab. Assessing it is key for prevention and helps design home rehab programs. Fatigue reduces movement speed, which can be determined by acceleration. Kinematic parameters such as acceleration are widely used to define fatigue in exercise [15]. KR-based video analysis algorithm has the advantages of convenience, high efficiency, and non-disturbance. But its validity and reliability of KR algorithm need to be determined before it can be utilized as a fatigue detection tool.

Bini confirmed that posture estimation technology can assess cycling motion and calculate lower limb features [16, 17]. By comparing with an inertial sensor unit (IMU) system to: (1) establish the feasibility of the KR for cycling movement analysis and (2) validate the recognition and analysis of different movement statuses based on the KR algorithm with information processing techniques. In this way, a convenient deep learning movement assessment method has been established, which is used to develop personalized assessment models and provides a straightforward method for rehabilitation assessment and training in home or community settings.

Methods

Participants

The appropriate sample size was determined using the GPower V.3.1 program. At least 17 participants were needed to achieve an 80% power and a 5% error rate in a two-tailed test. Twenty healthy college students (13 males and 7 females, age: 20.9 ± 2.0 years, height: 170.3 ± 9.8 cm, weight: 61.7 ± 11.8 kg, body mass index: 21.2 ± 3.3 kg/m^2) participated in this study. This study was approved by the Biomedical Research Ethics Review Committee of Fujian Medical University (Document No. (160) of 2022 FCM Ethics Review). Participants' informed consent was obtained.

The inclusion and exclusion criteria for this study are presented as follows:

Inclusion Criteria: 1. Participants must be in good physical health, with no history of significant chronic illnesses. This includes: Cardiovascular conditions (e.g., coronary heart disease, hypertension, arrhythmia), Respiratory disorders (e.g., chronic obstructive pulmonary disease, asthma), Neurological conditions (e.g., stroke), Endocrine diseases (e.g., diabetes), and Musculoskeletal issues (e.g., severe arthritis, post-operative recovery from joint replacement). 2.Participants must be capable of engaging in physical activities, as determined by the Physical Activity Readiness Questionnaire (2014 PAR-Q). 3.They must be able to: Understand and sign the informed consent form.Willingly participate in the study and adhere to the experimental protocol.Perform all

required tasks, including wearing a breathing mask, completing cycling exercise trials as instructed, and allowing for data collection.

Exclusion Criteria: Participants will be excluded if they meet any of the following conditions:

Underwent major surgery or experienced significant trauma within the past six months that could affect cardiopulmonary function or exercise ability; Have mental health disorders or cognitive impairments that hinder communication, comprehension, or cooperation during the experiment. Have a history of drug or alcohol misuse that significantly impacts cardiopulmonary function during physical activity; Are pregnant or breastfeeding; Exhibit allergies to the breathing mask materials or cannot tolerate its use; Have noticeable motor dysfunctions that prevent the safe performance of cycling exercises.

Experimental procedure

Participants should wear close-fitting and light-colored clothes for recognition of KR-based key body points. Figure 1 depicts the 17 key points recognized by the KR algorithm.

A stationary bike (BC22002, LeiKe magnetic exercise bike, China) cycling exercise was selected. IMUs (myomotion, NORAXON, USA) were positioned on the pelvis, bilateral thighs, shanks and feet to capture three-dimensional acceleration data at a sampling rate of 100 Hz. At the same time, an ordinary smartphone (K40, RedMi, China) was set up on a phone stand placed on the right side 2 m away from the right side of the subject and with a height of 1 m to record movement videos. The phone recorded two-dimensional coordinate displacement information of 17 human body keypoints using the KR algorithm at a frequency of 30 Hz. Participants sit on a 45 cm-high chair and maintain stillness for 10 s to collect baseline data. Then, participants performed a natural cycling exercise in a fixed position for 30 s, repeated thrice, with a 3 min rest between sets. The task was for participants to complete a 120s (the 0 to 2nd minutes) ride at Phase1-normal speed (pedaling frequency of approximately 50 rpm) and Phase 2-fast speed (pedaling frequency of approximately 80 rpm) for 120s (the 3rd to 4th minutes) on the stationary exercise bike for a total of 4 min, as shown in Fig. 2.

Index	Joint
1	Nose
2	Left Eye
3	Right Eye
4	Left Ear
5	Right ear
6	Left Shoulder
7	Right Shoulder
8	Left Elbow
9	Right Elbow
10	Left Wrist
11	Right Wrist
12	Left Hip
13	Right Hip
14	Left Knee
15	RIght Knee
16	Left Ankle
17	Right Ankle

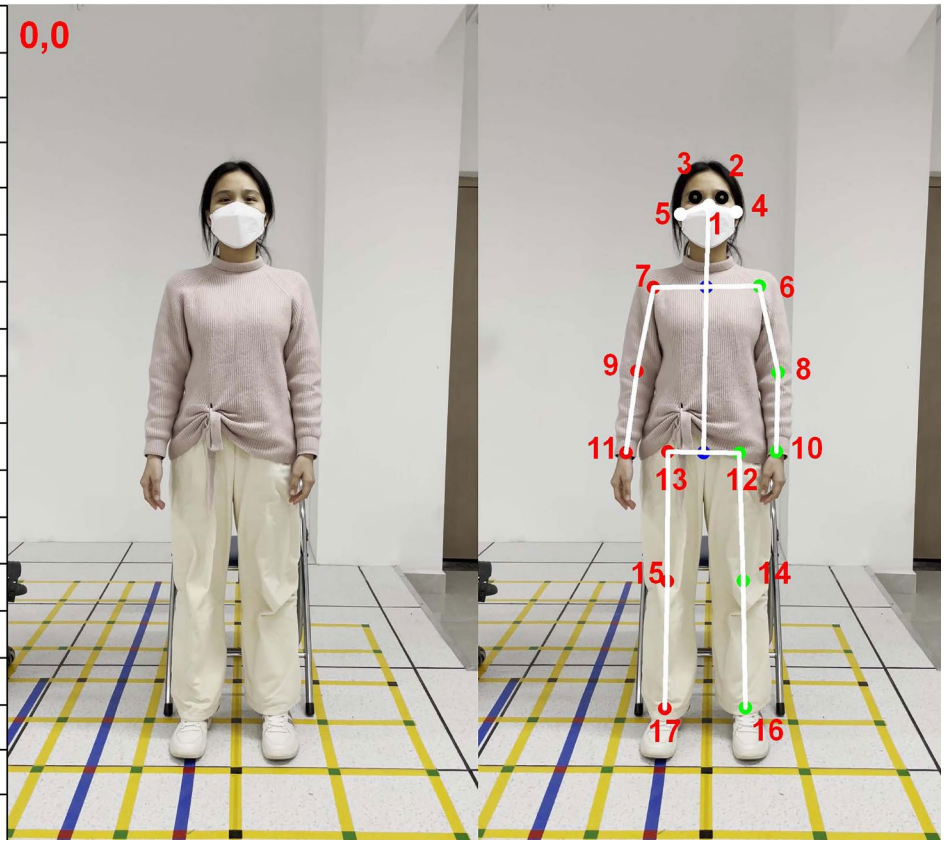

Fig. 1 The Keypoint RCNN calculates the 17 key points of the human body. The origin of the pixel coordinates is located in the top-left corner, denoted as (0,0). The row number of the vertical coordinate increases from top to bottom in an integer value, and the horizontal coordinate column number increases in an integer value from left to right

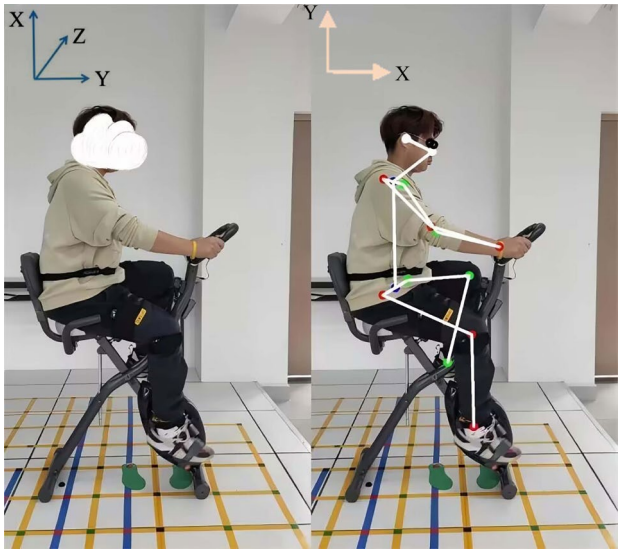

Fig. 2 A participant performed the exercise on a stationary bike. The three-axe coordinates on the left-low are the direction of the IMU sensor, and the two-axe coordinates on the right-low are the direction of KR. A smartphone captures a two-dimensional coordinate of 17 keypoints at a 1920×1080 resolution from a right-side view

Data processing

Multiscale entropy calculation

Sample entropy (*SE*) computes the presence of repeated data of any length in a time series to describe its complexity [18]. Costa et al. [13] expanded sample entropy and defined multiscale entropy (MSE) as the result of the continuous smoothing of a time series to quantify the complexity hidden in the signal. Smoothing is achieved by averaging the data points in a given nonoverlapping window. The complexity of the vertical acceleration data of the right knee during the movement process was assessed using the multiscale entropy (MSE) analysis in this study. The calculation of the MSE includes three processes: sequence coarse-graining, sample entropy calculation, and complexity index.

- **Sequence coarsening**: The time series is divided into multiple time scales to calculate the entropy values at different scales. Coarse-graining is calculated according to Eq. (1), where x_i is the original time series data points; $y_j^{(\tau)}$ is the new sequence, j is the data point in the new sequence; τ is the number of window data points, called the scale factor; and N is the size of the original data set. Coarse-graining means that the time series length decreases to N/τ as τ increases.

$$y_j^{(\tau)} = \frac{1}{\tau} \sum_{i=(j-1)\tau+1}^{j\tau} x_i \quad , \; 1 \leqslant j \leqslant \tfrac{N}{\tau} \tag{1}$$

- **Sample entropy calculation**: After coarse-graining the sequence, an *SE* value can be obtained for each scale [19]. The calculation procedure is described in detail below.

Step 1: Set the parameters of the data comparisons (m) and the tolerance (r).
It is generally recommended that m be set to 2 or 3 and r to 0.1 ~ 0.2 [20].

Step 2: Given a time series$\{x_{1\ldots\ldots}x_{m\ldots\ldots}x_i\}$, the number of comparisons is m, i.e., every m points form a group. Compare the first group$(x_1 \ldots x_m)$with every other group of m consecutive points. Calculate the maximum difference $d[x_i,x_j]$across all comparison groups with Eq. (2).

$$\begin{aligned} d\left[x_i, x_j\right] &= \max\left[\left|x_i + 1 - x_j + 1\right|\right], \\ & 1 \leq i \leq N - m, 1 \leq j \leq N - m \end{aligned} \tag{2}$$

Step 3: Compare $d[x_i,x_j]$ to r*SD, where SD represents the standard deviation of the original sequence. If $d[x_i,x_j]$ is smaller than r*SD, the two comparison groups are similar. Calculate the total number of similar occurrences, $n_{i(m)}$, and use Eq. (3) to calculate the probability, $C_{i(m)}$, of generating similar numbers.

$$C_{i(m)} = \frac{n_{i(m)}}{N-m}, 1 \leq i \leq N - m \tag{3}$$

Step 4: C_m represents the average value of $C_{i(m)}$, corresponding to the probability of groups comprising m points matching each other. Equation (4) describes the calculation method.

$$C_m = \frac{1}{N-m} \sum_{i=1}^{N-m} C_{i(m)} \tag{4}$$

Step 5: Increase the number of compared elements to $m+1$ and repeat the above steps. Obtain the cumulative number of similar occurrences, $n_{i(m+1)}$, and the corresponding probability, $C_{i(m+1)}$, calculated using Eq. (5). Denote the resulting average of $C_{i(m+1)}$ as C_{m+1}, and determine it using Eq. (6).

$$C_{i(m+1)} = \frac{n_{i(m+1)}}{N-m-1}, \; 1 \leqslant i \leqslant N - m - 1 \tag{5}$$

$$C_{m+1} = \frac{1}{N-m-1} \sum_{i=1}^{N-m-1} C_{i(m+1)} \tag{6}$$

Step 6: By integrating the sequence coarse-graining process and considering the scale factor τ, the calculation of

sample entropy involves taking the negative natural logarithm of the ratio of C_{m+1} to C_m. It is determined using Eq. (7).

$$SE(\tau, m, r) = -\ln(\frac{C_{m+1}}{C_m}) \tag{7}$$

- **Complexity Index** (***CI***): The relationship between sample entropy and τ is described by the MSE curve, with the complexity metric represented by the area under the curve, as illustrated in Fig. 3. Equation (8) exhibits the calculation method. τ_{max} is the optimal scale chosen based on the amount of data.

$$CI\left(\tau_{\max}, m, r\right) = \sum_{\tau=1}^{\tau_{\max}} SE(\tau, m, r) \tag{8}$$

The sampling rates of KR and IMU differ, resulting in varying data volumes. To ensure a fair comparison, this study employed the complexity index average (*CIA*) for analysis. However, the *CIA* does not include time information, making it unable to assess the complexity before and after status changes during the movement process. Therefore, in this study, the Y-axis acceleration signal of the right knee joint underwent STFT to identify the transition time points between movement statuses. Using these time points, the Y-axis acceleration signals for both KR and IMU of the right knee joint were segmented into Phase 1 and Phase 2. Subsequently, MSE calculations were conducted separately to derive *CIA*.

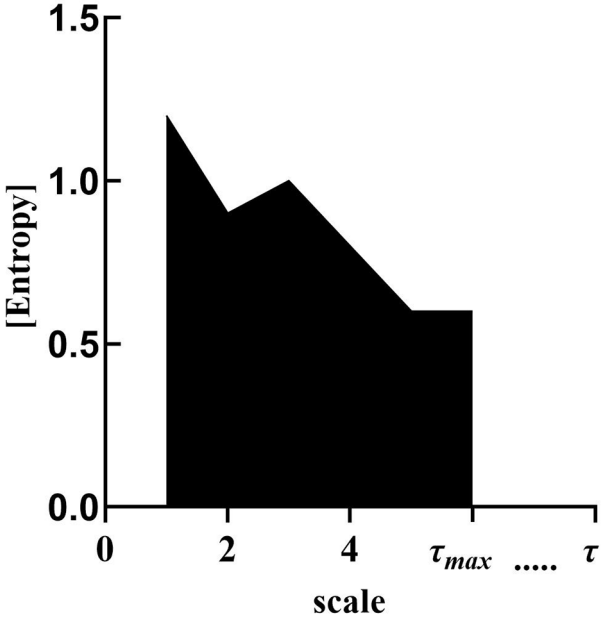

Fig. 3 The area under the MSE curve is defined as the complexity index. The horizontal coordinate represents the scale factor τ, and the vertical coordinate represents the sample entropy value for each scale

Data processing and analysis

The exercise process on the stationary exercise bike is mainly the active pedaling and stretching of the lower limbs, especially the flexion and extension of the knee joint as the main source of power. The study focused on analyzing the vertical direction data of the right knee joint, primarily due to obstruction caused by the human body. IMU system acquired acceleration data, defined as sensor values and measured in cm/sec². The units of acceleration obtained from KR differ from those of the IMU, making direct comparison unfeasible. According to the literature, the peak frequency can reflect different activity statuses of the human body [21]. So the acceleration data needs to be converted into frequency-domain features with FT and validated by a unified standard of time–frequency analysis. The mathematical operations of differentiation, filtering, FT, STFT, and MSE were conducted with the Visual Signal version 1.6 STD.

The flow chart for processing and analyzing KR algorithm data is illustrated in Fig. 4: (1) The data was normalized before analysis. (2) Displacement data from KR undergoes a 2nd derivative to derive pixel acceleration (defined as the KR value) in units of pixel/Sec^2. (3) A filtering operation was performed to remove noise from the data. (4) After obtaining the peak frequency of acceleration through FT, the *CIA* value was then obtained through MSE analysis and further analyzed and compared for correlation and differences. The results were presented in Tables 1 and 2. (5) Transition time points from Phase 1 to Phase 2 were identified using STFT and compared predetermined values, with outcomes presented in Table 3. (6) The data was partitioned into Phase 1 and Phase 2 based on the transition time points, and the corresponding *CIA* values were obtained, followed by *t*-tests, the results displayed in Table 4. The data processing workflow for IMU data was akin to KR data processing, except for the absence of 2nd derivative.

Statistical analysis

IBM SPSS Statistics version 26 was used for the statistical analyses. In evaluating the reliability of the KR algorithm, $ICC_{1,3}$ was utilized to compare the mean values of 30-second data over three trials to ascertain the intra-session consistency of the KR algorithm.

To assess the agreement and consistency of acceleration data collected by the two movement capture systems, Spearman's correlation, $ICC_{2,1}$was used. An ICC value can be interpreted as follows: values below 0.5 signify poor consistency, values between 0.5 and 0.75 indicate moderate consistency, values between 0.75 and 0.9 indicate good consistency and values exceeding 0.90

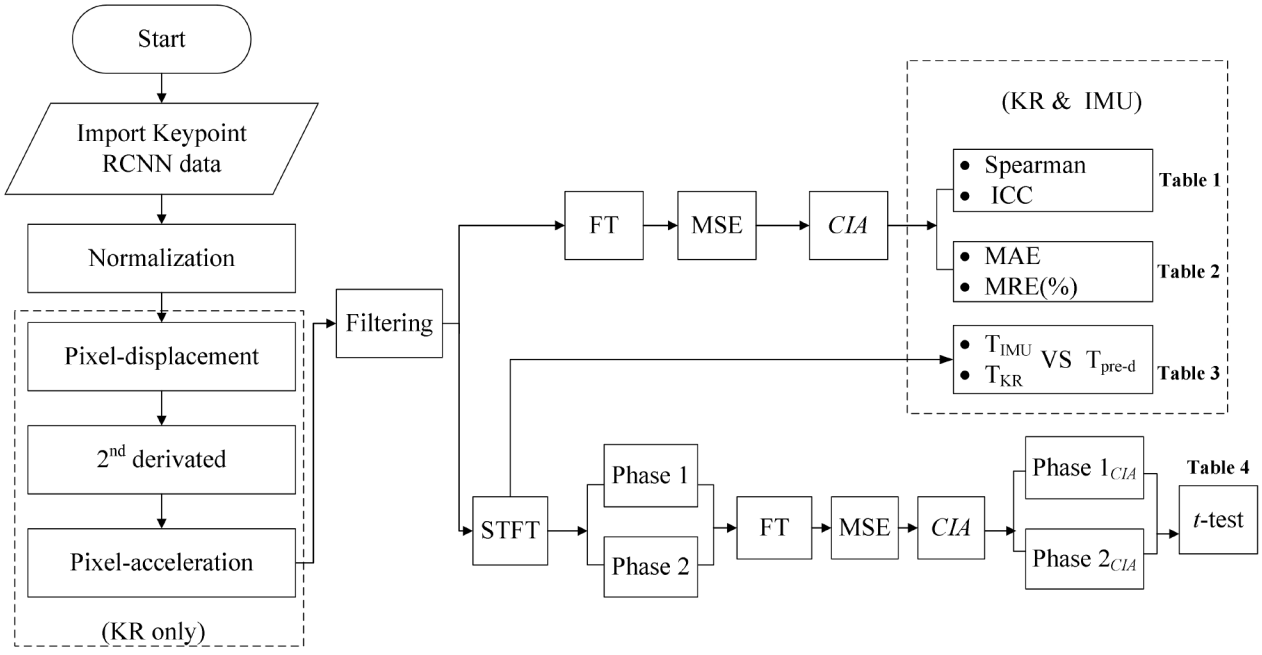

Fig. 4 The flow chart of the KR algorithm data analysis. Normalization was based on the average value of the data from the right knee key point remaining still for 10 s, and it reseted the data for the KR algorithm. Data noise was attenuated using an FIR filter with a 3 Hz cutoff frequency. Selecting an appropriate window function and time-frequency resolution is essential for STFT to depict the data characteristics accurately. The Hanning function was selected as the window function for the calculation parameters, and the window length was 0.8. T_{IMU} and T_{KR} represent the transition time points derived from IMU and KR

Table 1 The correlation and consistency between the data from the KR and IMU

	Peak frequency	MSE
IMU(mean ± sd)	1.33 ± 0.33	0.51 ± 0.07
KR(mean ± sd)	1.33 ± 0.33	0.48 ± 0.07
Correlation coefficient(95% confidence interval)	1.000**	0.881**(0.749 ~ 1.000)
$ICC_{2,1}$ (95% confidence interval)	1.000**(1 ~ 1)	0.865**(0.368 ~ 0.957)

** $p < 0.01$

Table 2 The data error metrics of the IMU and KR

	Peak frequency(Hz)		CIA	
	MAE	MRE (%)	MAE	MRE (%)
Right-knee Y	0.001	0.00	0.040	7.67

Table 3 The STFT of all subjects was subjected to the KR algorithm with IMU measurement data for the transition time point of movement status change captured and analyzed with the results of error analysis with Tpre-d = 120 ± 0s

	T_{IMU} (s)	T_{KR} (s)
M ± SD	120.27 ± 0.32	120.28 ± 0.37
MAE	0.32	0.37
MRE	0.00%	0.23%

Table 4 *CIA* values and *t*-test results for the two movement statuses of phase 1 and phase 2

	IMU	KR
$Phase1_{CIA}$	0.45 ± 0.13	0.40 ± 0.11
$Phase2_{CIA}$	0.34 ± 0.19	0.34 ± 0.19
p-value	0.003	0.03

suggest excellent consistency [22]. Furthermore, a correlation coefficient greater than 0.7 indicates a strong correlation [23].

The differences in the data obtained using the two methods were compared using the mean absolute error (MAE) and the mean relative error (MRE), as detailed in Eqs. (9) and (10). The variables X and Y both have a sample size of n points. Their MAE and MRE are defined as follows:

$$MAE = \frac{\sum_{i=1}^{n} |Xi - Yi|}{n} \tag{9}$$

$$MRE = \frac{1}{n} \sum \frac{|Xi - Yi|}{Yi} \tag{10}$$

The variables X_i and Y_i represent the i-th samples of X and Y, respectively, where i is the element index from 1 to n.

The experiment verified whether the movement status transition time points captured by the two methods correspond to the preset occurrence at 120s and whether other change thresholds occurred during the exercise. The *t*-tests were performed to analyze the variances in acceleration *CIA* corresponding to different pedaling speed statuses between the KR algorithm and IMU measurements. A value of $p < 0.05$ indicated that the difference was statistically significant.

Results

Captured the peak frequency of knee joint movement based on KR and IMU

The results demonstrated that during three repetitions of cycling (with the mean and standard deviation being 0.75 ± 0.20, 0.78 ± 0.20, and 0.80 ± 0.20 respectively), the peak acceleration frequency had excellent intra-session reliability ($ICC_{1,3}$ = 0.988, 95% CI = 0.976–0.995).

Figure 5 presents original acceleration signals in time series from a representative subject and their corresponding Fourier transform (FT) plots. The FT plot depicts the peak frequency of acceleration, and the peaks indicate a concentration. They also suggest consistent frequency changes of accelerations obtained by the IMU and KR.

Correlation and consistency analysis

Table 1 provides a detailed comparison of the peak frequency and *CIA* consistency between the KR and IMU systems. Results indicated a strong correlation ($r > 0.7$) and good consistency ($ICC_{2,1} > 0.8$) of peak frequency and *CIA* estimated by the two systems.

The data of error analysis

As shown in Table 2, peak frequency and *CIA* values calculated by the KR demonstrate small MAE and MRE when compared with those of the IMUs (MAE = 0.001 and 0.040, MRE = 0.00% and 7.67%, respectively), confirming that data collected by the KR and the IMU are consistent.

Feasibility of integrating SFTF and MSE

Figure 6 shows the STFT plot of IMU and KR data for a participant. It can be observed that the frequency band of 6(a) IMU or 6(b) KR transformed from a narrow and light-colored band for the normal speed Phase1 to a wide and dark-colored band for the fast speed Phase2 at time 120 s. The color shades in Fig. 6 represent the intensity level. The higher the frequency of the movement, the higher the energy intensity. The colors of the frequency segments in Fig. 6(a) and (b) both become darker and denser after 120s, which shows that the STFT corresponds to the data before 120s as Phase 1 and after 120s as Phase 2.

The transition time point from Phase 1 to Phase 2 of this experiment was pre-defined at 120s (T_{pre-d} = 120s). Table 3 shows the comparison results of estimated phase transition time points using IMU (T_{IMU}) and KR (T_{KR}) and the T_{pre-d}. Results demonstrate that both of the two systems showed minimal errors (T_{IMU} = 120.27 ± 0.32s, MAE = 0.32, MRE = 0.00%; and T_{KR} = 120.28 ± 0.37s, MAE = 0.37, MRE = 0.23%, respectively).

Table 4 shows the *t*-test results of the *CIA* values of the two movement phases (Phase1-normal speed, $Phase1_{CIA}$, Phase2-fast speed and $Phase2_{CIA}$) measured by IMU and KR algorithms. $Phase1_{CIA}$ and $Phase2_{CIA}$ estimated by both the IMU and KR systems showed significant differences (p = 0.003 and 0.03, respectively).

Discussion

Deep learning-based pose estimation algorithms significantly lower the cost of implementing motion capture systems. Moreover, deep learning technology requires no professional equipment, making remote home-based motion capture and analysis applicable [24]. We employed the KR algorithm to track the trajectories of cycling movements and, for the first time, applied signal processing techniques based on MSE to analyze frequency metrics associated with the motion status. The KR algorithm demonstrated good reliability and validity compared to the referential IMU system. Specifically, the integration of the KR algorithm with *CIA* enables precise detection of various movement statuses, ensuring the effective application of deep learning technology in movement assessment.

The KR-based movement capture method demonstrates excellent intra-session reliability, suggesting it can maintain stability and obtain accurate data among various measurement sessions. A reliable measurement tool could also be applied for long-term functional ability progression. Moreover, the movement data derived from the KR algorithm demonstrated good consistency with the referential IMU system and minimal measurement error across various speeds of pedaling, further validating the effectiveness of the KR algorithm. The deep learning KR algorithm can potentially serve as an evaluation tool for movement screening in a home-based setting. The other commonly used pose estimation algorithms, for example, OpenPose, demonstrated comparative reliability ($ICC_{1,3}$ = 0.92–0.96) and validity ($ICC_{2,1}$ = 0.80) [25]. The KR algorithm has improved both in terms of stability of its own acquisitions and data accuracy.

We employed MSE with time-frequency methods (FT and STFT) to analyze diverse acceleration peak frequencies. Our research found that STFT can provide detailed temporal information on movement status transitions, and MSE can identify changes in complexity when the transition occurs. These findings establish a theoretical

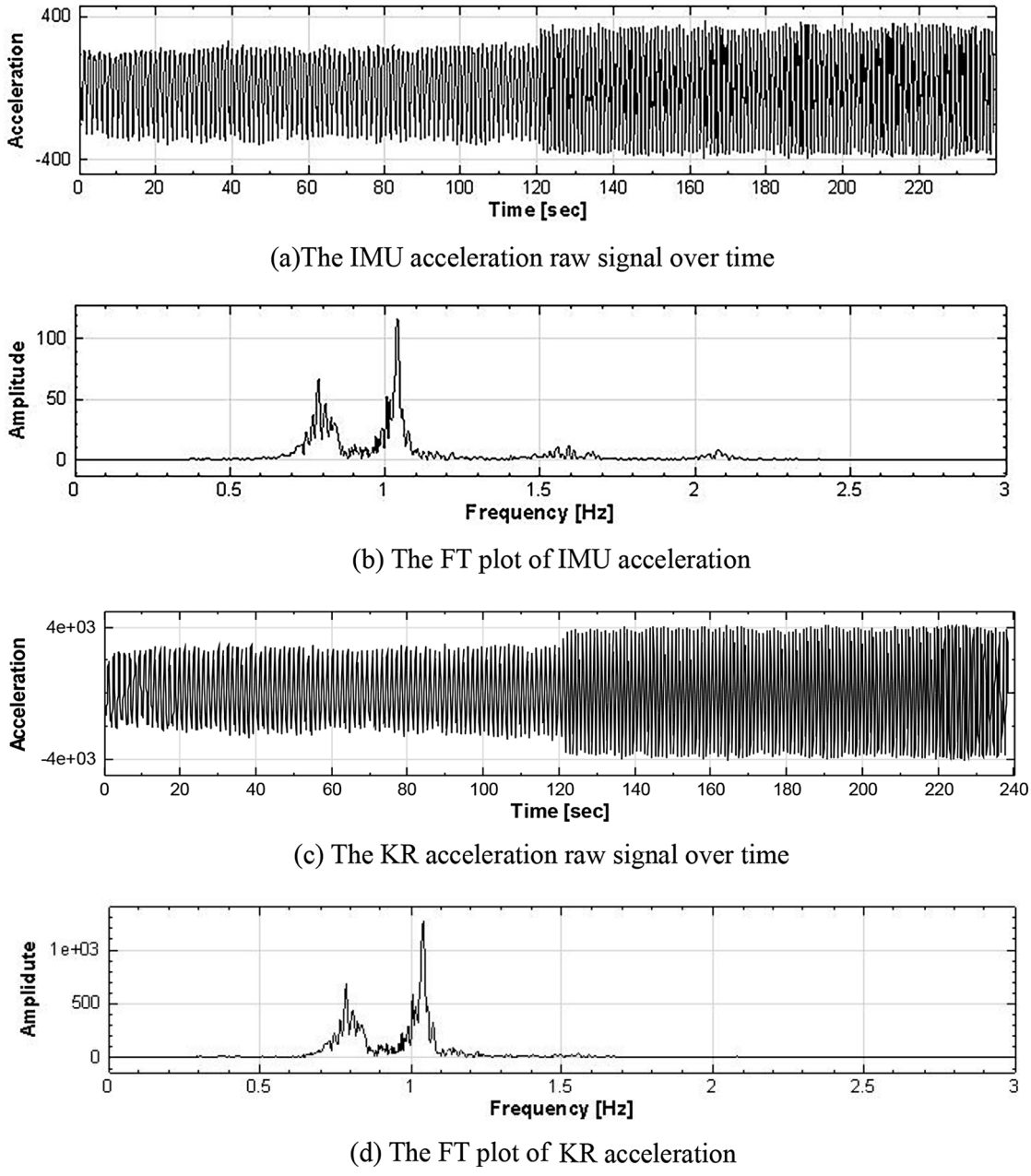

Fig. 5 The acceleration raw signal over time in the right knee's Y-direction and its FT plot of a participant. Plots (**a**) and (**c**) depicted the original IMU and KR algorithm-measured acceleration signals, while plots (**b**) and (**d**) displayed their respective FT plots. These plots illustrate that the subject demonstrated two distinct segments of pedaling acceleration frequency during the exercise, occurring at approximate frequency ranges of 0.65–0.90 Hz and 0.95–1.10 Hz

foundation for detecting fatigue during exercise. By integrating the KR algorithm with the signal processing techniques, we have developed a novel deep learning movement assessment method. This innovation provides valuable insights for future research on personalized movement assessment models.

Figure 6 depicts the cycling acceleration frequency and amplitude changing accompanying movement status transitions. Higher acceleration amplitude suggests more remarkable changes during pedaling. The KR algorithm exhibited consistent frequency ranges and peak performances in its respective FT images compared to the IMU system. We also observed that the amplitude obtained with the KR was greater than the amplitude of the IMU. This is likely related to the pixel displacement collected by the KR. Compared with the actual displacement

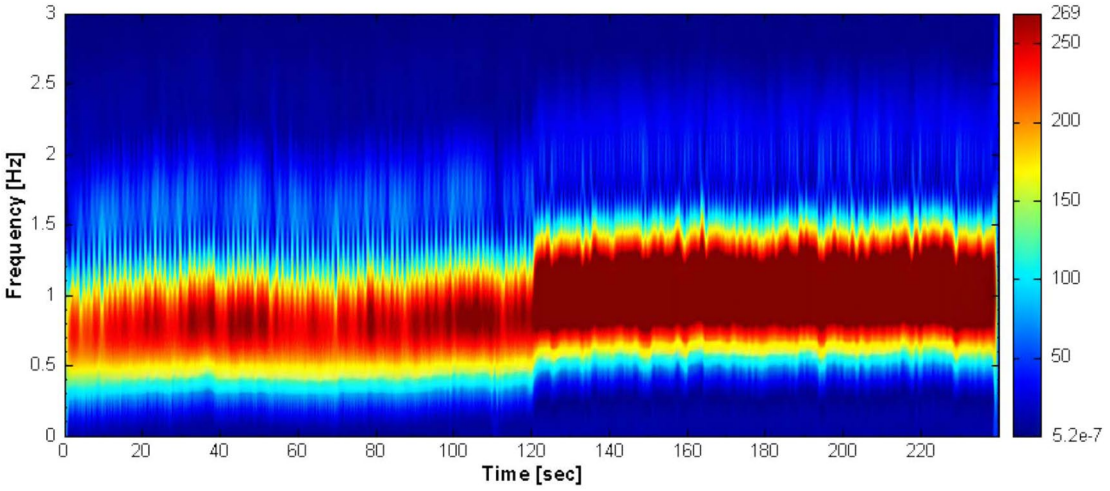

(a) The STFT image of the IMU

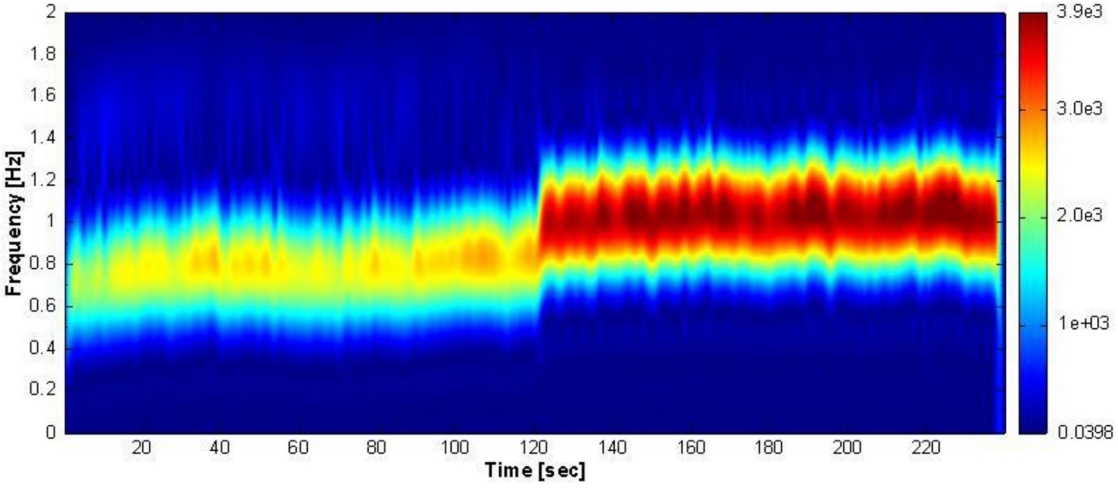

(b) The STFT image of the KR

Fig. 6 The STFT images of IMU and KR right-knee Y-direction acceleration data of a subject. The horizontal coordinate is time, the left vertical axis is frequency value, and the right vertical axis is energy intensity value. It indicates the energy magnitude of the signal at a specific time and frequency. The colors in the image represent energy intensity. The darker the color, the higher the frequency of exercise and the greater the energy intensity. From (**a**) and (**b**), both Phase 2 color are darker than those in Phase 1

measured by the IMU, the pixel displacement had a longer moving distance on the image. Peak frequency analysis can directly analyze whether the spectrum of two signals is equivalent. It does not need to be converted into the same unit and does not impact the experiment.

The crucial information of 'time' is added to the STFT image, which can assist therapist to understand the time point of a frequency change, and the darkness of the spectrum's color represents the energy intensity level. It is worth noting that the color of the STFT image of the KR was lighter than the IMU, which is related to the sampling frequency. In the same period, if the sampling frequency is high, the amount of data will be extensive, and the color of the image will be darker. STFT can accurately capture the time when the speed changes from normal to fast, which means that STFT can capture the status transition thresholds related to speed change during actual movement. For instance, if a participant shows physical fatigue and movement change (speed or acceleration) during exercise, the fatigue point can be determined through an STFT image. This can become an essential basis for individualized rehabilitation training programs. In addition, the MSE complexity was calculated separately for the acceleration signals in the two movement statuses, and the *t*-test results were all significant. MSE and STFT technology can distinguish different movement statutes and capture change thresholds, respectively. As a result, we are integrating the KR algorithm

and signal processing technology to propose a practical method to analyze movement status conveniently.

Furthermore, the complexity of Phase 1 was higher than that of Phase 2, indicating that the complexity is higher during the normal speed movement process. This is related to the fact that the human body quickly enters an anaerobic exercise status when performing fast or intense exercise. Physiological complexity decreases if the body's muscles or cardiorespiratory system fatigue. Therefore, using normal training speed as the daily training condition is more suitable for delaying the onset of exercise-induced fatigue.

In this study, the KR algorithm was utilized for movement capture and analysis in a typical cycling exercise for rehabilitation. Theoretically, the KR algorithm has the potential to be applied in the advanced field of rehabilitation medicine. Future applications include ergonomic posture analysis, sports injury risk screening, gait analysis, and fall detection. It can be leveraged to develop semi-automated diagnosis and treatment systems or integrated with virtual reality to create interactive rehabilitation robots. The proposed method is applicable to sports training, dance instruction, and similar activities, enabling the evaluation of movement quality and the facilitation of dynamic health management.

This study presents several significant advantages over existing research. First, it employs a stationary exercise bicycle, which is not only cost-effective and widely accessible but also highly user-friendly. Second, the KR algorithm eliminates the need for wearable accessories, allowing data to be conveniently collected using only a mobile phone. This feature makes it particularly suitable for both domestic and community settings, enhancing convenience. Third, the integration of the KR algorithm with signal processing techniques introduces a novel motion assessment method characterized by objectivity, relatively straightforward requirements, and strong practical applicability. Lastly, this methodology can be extrapolated to other sports activities, presenting a novel avenue for motion evaluation and analysis.

This study has three limitations: (1) The KR algorithm is a two-dimensional analysis method. Its accuracy would be reduced when evaluating three-dimensional movement tasks. Measurement error correction algorithms need to be developed in future studies. (2) Only young, healthy adults were involved in this study. Considering the clinical utility of the KR algorithm, it is necessary to recruit more clinical populations to further verify its reliability and validity [25]. (3)This method is currently limited to analyzing the motion trajectories of stationary bicycles. Its potential application to more complex sports, such as ball games, remains uncertain and warrants further investigation.

Conclusion

The main finding of this study is that the results estimated by the KR and IMU are consistent, which can also be found in other deep learning algorithm-validating studies [26]. The findings suggest that the deep learning-based Keypoint RCNN (KR) algorithm provides sufficient accuracy for movement analysis. Additionally, we have introduced a novel movement assessment method by integrating the KR algorithm with signal processing techniques. This deep learning-based movement status assessment technology has been successfully applied to exercise movement analysis and holds potential for large-scale community rehabilitation screening and other public health-related applications.

Abbreviations

KR	Keypoint RCNN
ICC	Intraclass correlation coefficient
CIA	The complexity index average
FT	Fourier Transform
STFT	Short-Time Fourier Transform
SE	Sample entropy
MSE	Multi-scale Entropy
IMU	Inertial sensor unit
CI	Complexity Index
MAE	Mean Absolute Error
MRE	Mean Relative Error

Acknowledgements

We thank all of the participants who participated in the study. We also thank the Rehabilitation Engineering Research Center of Fujian Province Universities for providing the research site and equipment.

Author contributions

C. P designed the original study; C. P directed the experiments; YC. H performed the experiments; YC. H and F. Ywere responsible for data collection and analysis; YC. H, C. P, and YH. Z and YR. M reviewed the relevant literature and interpreted the obtained information; YC. H drafted the manuscript; C. P, and YH. Z and YR. M Marevised the manuscript. All authors have read and approved the final manuscript.

Funding

This study was supported by the following projects: The Upper-Level Project of the Natural Science Foundation of Fujian Province (No. 2020J01653 and No. 2023J01323); Research Start-up Project for High-level Talents of Fujian Medical University (No. XRCZX2019011and XRCZ2022010); Special Project on Assistive Devices for the Disabled of the China Disabled Persons' Federation (No. 2023CDPFAT-02); Fujian Special Financial Project for Research (22SCZZX009).

Data availability

The datasets used and/or analysed during the current study are available from the first author upon request.

Declarations

Ethics approval and consent to participate

This study was approved by the Biomedical Research Ethics Review Committee of Fujian Medical University (Document No. (160) of 2022 FCM Ethics Review). All participants filled out the informed consent form. All experiments were performed in accordance with relevant guidelines and regulations.

Consent for publication

In this study, all participants were older than 18 years. we have obtained written informed consent from their for the publication of recognizable images (figure no. 1 & 2) with other data details.

Competing interests
The authors declare no competing interests.

Received: 4 February 2024 / Accepted: 16 December 2024
Published online: 11 February 2025

References

1. Huo CC, Zheng Y, Lu WW, et al. Prospects for intelligent rehabilitation techniques to treat motor dysfunction. Neural Regen Res. 2021;16(2):264–9. https://doi.org/10.4103/1673-5374.290884.
2. Lu L, Tan Y, Klaic M, et al. Evaluating Rehabilitation Progress using motion features identified by machine learning. IEEE Trans Biomed Eng. 2021;68(4):1417–28. https://doi.org/10.1109/TBME.2020.3036095.
3. Chang YJ, Chen SF, Huang JD. A Kinect-based system for physical rehabilitation: a pilot study for young adults with motor disabilities. Res Dev Disabil. 2011;32(6):2566–70. https://doi.org/10.1016/j.ridd.2011.07.002.
4. Liao Y, Vakanski A, Xian M. A Deep Learning Framework for assessing Physical Rehabilitation exercises. IEEE Trans Neural Syst Rehabil Eng. 2020;28(2):468–77. https://doi.org/10.1109/TNSRE.2020.2966249.
5. Cao Z, Hidalgo G, Simon T, Wei SE, Sheikh Y, OpenPose. Real-time multi-person 2D pose estimation using part affinity fields. IEEE Trans Pattern Anal Mach Intell. 2021;43(1):172–86. https://doi.org/10.1109/TPAMI.2019.2929257.
6. Shi Q, Zhang H-B, Dong L-J, et al. Vision Skeleton trajectory based motion Assessment System for healthcare rehabilitation. J Eng. 2020;2020(9):805–8. https://doi.org/10.1049/joe.2019.1316.
7. Chen W, Jiang Z, Guo H, et al. Fall detection based on key points of human-skeleton using OpenPose. Symmetry. 2020;12(5):744. https://doi.org/10.3390/sym12050744.
8. Liu L, Qing MA, Chen S et al. Tai chi movement recognition method based on deep learning algorithm. Math Probl Eng. 2022;7974669. https://doi.org/10.1155/2022/7974669
9. Sato K, Nagashima Y, Mano T, Iwata A, Toda T. Quantifying normal and parkinsonian gait features from home movies: practical application of a deep learning-based 2D pose estimator. PLoS ONE. 2019;14(11):e0223549. https://doi.org/10.1371/journal.pone.0223549.
10. He K, Gkioxari G, Dollar P, Girshick R, Mask R-CNN. IEEE trans pattern anal mach intell. 2020;42(2):386–97. https://doi.org/10.1109/TPAMI.2018.2844175.
11. Takeda I, Yamada A, Onodera H. Artificial Intelligence-assisted motion capture for medical applications: a comparative study between markerless and passive marker motion capture. Comput Methods Biomech Biomed Engin. 2021;24(8):864–73. https://doi.org/10.1080/10255842.2020.1856372.
12. Inturi AR, Manikandan VM, Kumar MN, Wang S, Zhang Y. Synergistic integration of skeletal kinematic features for vision-based fall detection. Sens (Basel). 2023;23(14):6283. https://doi.org/10.3390/s23146283.
13. Costa M, Goldberger AL, Peng CK. Multiscale entropy analysis of complex physiologic time series. Phys Rev Lett. 2002;89(6):068102. https://doi.org/10.1103/PhysRevLett.89.068102.
14. Zhao J, She J, Fukushima EF, Wang D, Wu M, Pan K. Muscle fatigue analysis with optimized complementary ensemble empirical mode decomposition and multi-scale envelope spectral entropy. Front Neurorobot. 2020;14:566172. https://doi.org/10.3389/fnbot.2020.566172.
15. Marotta L, Scheltinga BL, van Middelaar R, et al. Accelerometer-based identification of fatigue in the Lower limbs during Cyclical Physical Exercise: a systematic review. Sens (Basel). 2022;22(8):3008. https://doi.org/10.3390/s22083008.
16. Bini RR, Serrancoli G, Santiago PRP, Pinto A, Moura F. Validity of neural networks to determine body position on the bicycle. Res Q Exerc Sport. 2023;94(4):905–12. https://doi.org/10.1080/02701367.2022.2070103.
17. Bini RR, Serrancoli G, Santiago PRP, Pinto A, Moura F. Criterion validity of neural networks to assess lower limb motion during cycling. J Sports Sci. 2023;41(1):36–44. https://doi.org/10.1080/02640414.2023.2194725.
18. Richman JS, Moorman JR. Physiological time-series analysis using approximate entropy and sample entropy. Am J Physiol Heart Circ Physiol. 2000,278(6):H2039-H2049. https://doi.org/10.1152/ajpheart.2000.278.6.H2039
19. Duarte M, Sternad D. Complexity of human postural control in young and older adults during prolonged standing. Exp Brain Res. 2008;191(3):265–76. https://doi.org/10.1007/s00221-008-1521-7.
20. Pincus SM. Approximate entropy as a measure of system complexity. Proc Natl Acad Sci U S A. 1991;88(6):2297–301. https://doi.org/10.1073/pnas.88.6.2297.
21. Pfister A, West AM, Bronner S, Noah JA. Comparative abilities of microsoft kinect and Vicon 3D motion capture for gait analysis. J Med Eng Technol. 2014;38(5):274–80. https://doi.org/10.3109/03091902.2014.909540.
22. Koo TK, Li MY. A Guideline of Selecting and Reporting Intraclass Correlation Coefficients for Reliability Research. J Chiropr Med. 2016;15(2):155–63. https://doi.org/10.1016/j.jcm.2016.02.012
23. Schober P, Boer C, Schwarte LA. Correlation coefficients: appropriate use and interpretation. Anesth Analg. 2018;126(5):1763–8. https://doi.org/10.1213/ANE.0000000000002864.
24. Washabaugh EP, Shanmugam TA, Ranganathan R, Krishnan C. Comparing the accuracy of open-source pose estimation methods for measuring gait kinematics. Gait Posture. 2022;97:188–95. https://doi.org/10.1016/j.gaitpost.2022.08.008.
25. Ota M, Tateuchi H, Hashiguchi T, et al. Verification of reliability and validity of motion analysis systems during bilateral squat using human pose tracking algorithm. Gait Posture. 2020;80:62–7. https://doi.org/10.1016/j.gaitpost.2020.05.027.
26. Yamamoto M, Shimatani K, Hasegawa M, Kurita Y, Ishige Y, Takemura H. Accuracy of temporo-spatial and lower Limb Joint Kinematics parameters using OpenPose for various gait patterns with orthosis. IEEE Trans Neural Syst Rehabil Eng. 2021;29:2666–75. https://doi.org/10.1109/TNSRE.2021.3135879.

Publisher's note